Figure S1

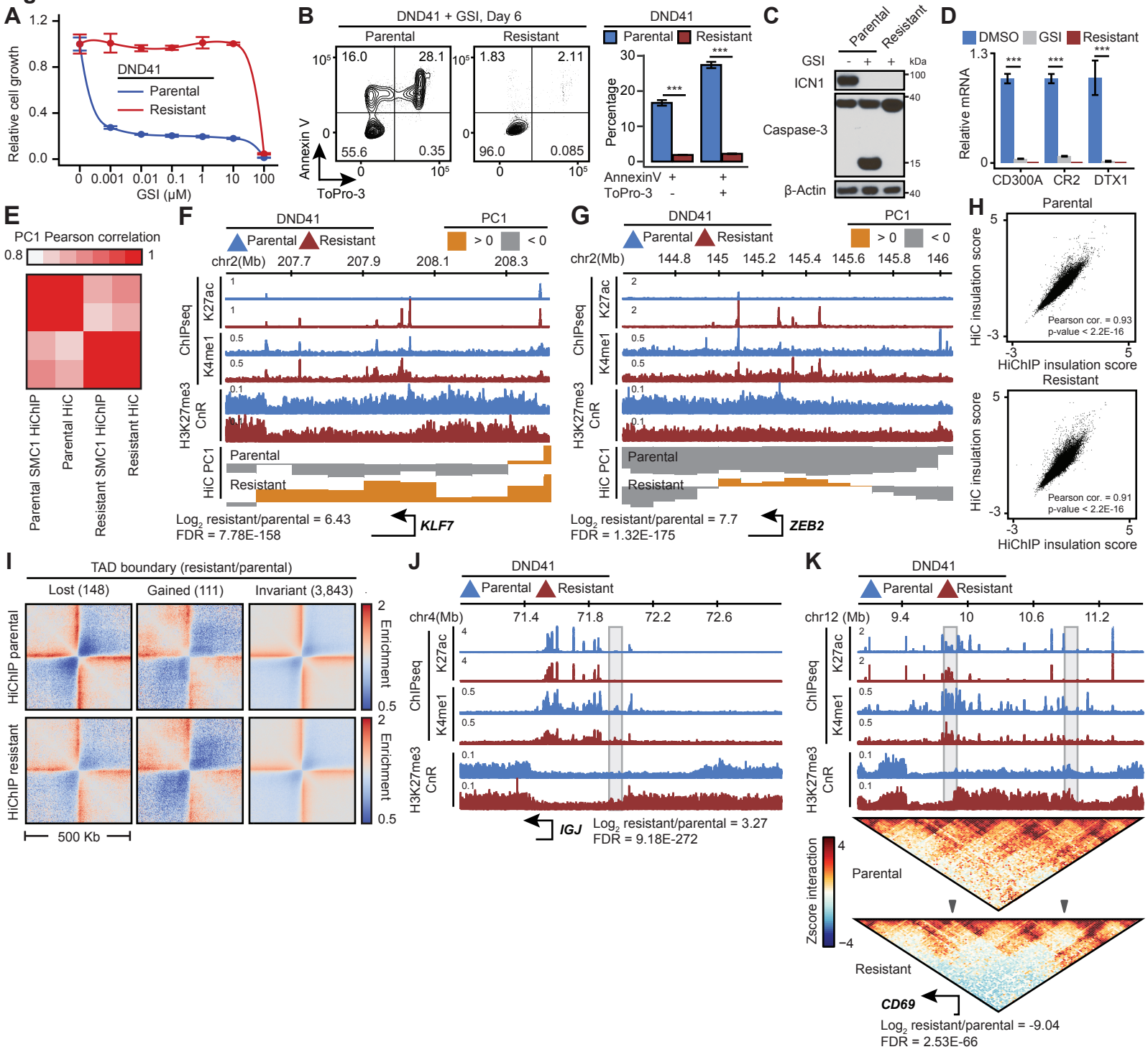
A
Relative cell growth
DND41
Parental
Resistant
GSI (μM)
B
DND41 + GSI, Day 6
Parental
Resistant
16.0
28.1
55.6
0.35
1.83
2.11
96.0
0.085
Annexin V
ToPro-3
DND41
Parental
Resistant
Percentage
AnnexinV
ToPro-3
C
Parental
Resistant
GSI
kDa
ICN1
Caspase-3
β-Actin
D
DMSO
GSI
Resistant
Relative mRNA
CD300A
CR2
DTX1
E
PC1 Pearson correlation
Parental SMC1 HiChIP
Parental HiC
Resistant SMC1 HiChIP
Resistant HiC
F
DND41
Parental
Resistant
PC1
chr2(Mb)
ChIPseq
K27ac
K4me1
H3K27me3
CnR
HiC PC1
Parental
Resistant
Log2 resistant/parental = 6.43
FDR = 7.78E-158
KLF7
G
DND41
Parental
Resistant
PC1
chr2(Mb)
Log2 resistant/parental = 7.7
FDR = 1.32E-175
ZEB2
H
Parental
HiC insulation score
HiChIP insulation score
Pearson cor. = 0.93
p-value < 2.2E-16
Resistant
Pearson cor. = 0.91
p-value < 2.2E-16
I
TAD boundary (resistant/parental)
Lost (148)
Gained (111)
Invariant (3,843)
HiChIP parental
HiChIP resistant
Enrichment
500 Kb
J
DND41
Parental
Resistant
chr4(Mb)
ChIPseq
K27ac
K4me1
H3K27me3
CnR
IGJ
Log2 resistant/parental = 3.27
FDR = 9.18E-272
K
DND41
Parental
Resistant
chr12 (Mb)
ChIPseq
K27ac
K4me1
H3K27me3
CnR
Zscore interaction
Parental
Resistant
CD69
Log2 resistant/parental = -9.04
FDR = 2.53E-66

Figure S1: GSI-resistant T-ALL tolerates high GSI dosage and reorganizes its chromatin. Related to Figure 1.

A: Relative cell growth (CellTiter-glo) of parental and GSI-resistant DND41 cells treated with the indicated doses of GSI for 6 days, showing that 10 nM GSI was sufficient to kill 70% of parental DND41 in 6 days, yet more than 90% of the GSI-resistant DND41 cells remained viable in 10 μM GSI. Representative experiment of 3 independent biological replicates with 5 technical replicates per dose.

B: Flow cytometry plots (left) and quantification (right) of cell apoptosis and death measured by Annexin V and ToPro-3 staining. Parental and GSI-resistant DND41 cells were treated with 125nM GSI for 6 days. Representative experiment of 3 independent biological replicates with 3 technical replicates. Student's t-test p-values: *** $p < 1E-7$.

C: Immunoblot showing that inhibition of intracellular NOTCH1 (ICN1) for 6 days induces apoptosis in parental DND41 cells measured by cleaved Caspase-3. GSI-resistant cells are not apoptotic in the absence of ICN1. β-Actin is a loading control.

D: qRT-PCR showing repression of known Notch target genes (Ryan et al., 2017) in GSI-treated parental and GSI-resistant DND41. Treatment same as B. Student's t-test p-values: *** $p = 0$.

E: Pairwise Pearson correlation between the PC1 values calculated in parental and GSI-resistant HiC and SMC1 HiChIP of contact correlation matrices.

F, G: ChIP-seq and Cut&Run tracks showing gain of active histone marks H3K27ac and H3K4me1, and loss of repressive chromatin mark H3K27me3 at the T cell proliferation regulator KLF7 (Flotho et al., 2007; Schuettpelz et al., 2012) (F) and the T-ALL-associated transcription factor ZEB2 (De Coninck et al., 2019) (G) loci. The PC1 values of HiC contact correlation matrices in parental and GSI-resistant cells show compartment switching from B (<0) to A (>0) (see STAR Methods). Bottom track indicating gene positions, expression fold changes and FDRs as determined by DESeq2.

H: Scatter plots showing highly correlated insulation scores calculated with SMC1 HiChIP and HiC contact matrices in parental (left) and GSI-resistant (right) DND41.

I: Pileup plots depicting normalized SMC1 HiChIP contact frequencies at DND41 TAD boundaries in parental (top) and GSI-resistant (bottom) cells where the boundary insulation potentials are decreased (left), increased (middle) or invariant (right) in the GSI-resistant cells. Each boundary was padded with 1 Mbp flanking regions on both sides. Resolution: 5 Kbp.

J: ChIP-seq and Cut&Run tracks showing segregation of active and repressive histone marks at the gained TAD boundary, marked by the gray box, near *IGJ* in GSI-resistant cells.

K: Top: ChIP-seq and Cut&Run tracks showing loss of active histone marks H3K27ac and H3K4me1 and gain of repressive histone mark H3K27me3 at the *CD69* locus. Bottom: Normalized contact matrices in parental and GSI-resistant cells showing two TAD boundaries (grey arrows and boxes) are strengthened in the GSI-resistant cells encompassing the gained H3K27me3.

Figure S2

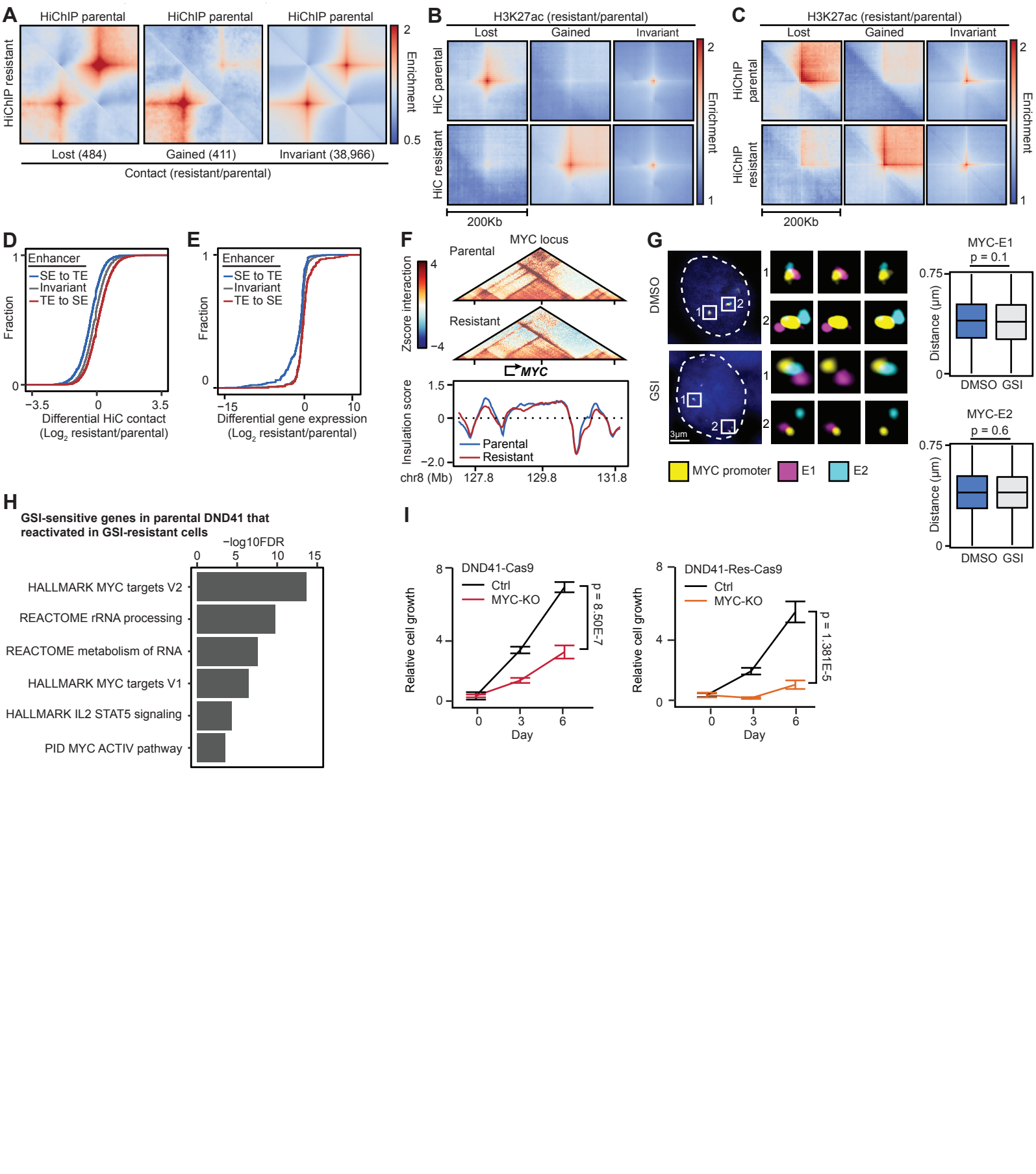
A
HiChIP parental
HiChIP parental
HiChIP parental
HiChIP resistant
Enrichment
2
0.5
Lost (484)
Gained (411)
Invariant (38,966)
Contact (resistant/parental)
B
H3K27ac (resistant/parental)
Lost
Gained
Invariant
HiC parental
HiC resistant
Enrichment
2
1
200Kb
C
H3K27ac (resistant/parental)
Lost
Gained
Invariant
HiChIP parental
HiChIP resistant
Enrichment
2
1
200Kb
D
Enhancer
SE to TE
Invariant
TE to SE
Fraction
1
0
−3.5
0
3.5
Differential HiC contact
(Log2 resistant/parental)
E
Enhancer
SE to TE
Invariant
TE to SE
Fraction
1
0
−15
0
10
Differential gene expression
(Log2 resistant/parental)
F
MYC locus
Parental
Resistant
Zscore interaction
4
−4
MYC
Insulation score
1.5
0
−2.0
Parental
Resistant
chr8 (Mb)
127.8
129.8
131.8
G
DMSO
GSI
1
2
3μm
MYC promoter
E1
E2
MYC-E1
p = 0.1
Distance (μm)
0.75
0
DMSO GSI
MYC-E2
p = 0.6
Distance (μm)
0.75
0
DMSO GSI
H
GSI-sensitive genes in parental DND41 that reactivated in GSI-resistant cells
−log10FDR
0
5
10
15
HALLMARK MYC targets V2
REACTOME rRNA processing
REACTOME metabolism of RNA
HALLMARK MYC targets V1
HALLMARK IL2 STAT5 signaling
PID MYC ACTIV pathway
I
DND41-Cas9
Ctrl
MYC-KO
p = 8.50E-7
Relative cell growth
8
4
0
0
3
6
Day
DND41-Res-Cas9
Ctrl
MYC-KO
p = 1.381E-5
Relative cell growth
8
4
0
0
3
6
Day

Figure S2: Differential enhancer activities correlate with differential loops in GSI-resistant T-ALL. Related to Figure 2.

A: Pileup plots of normalized SMC1 HiChIP contact maps in parental (top) and GSI-resistant (bottom) cells centered around the long-range contacts with decreased (left), increased (middle) or invariant (right) interaction frequencies in GSI-resistant compared to parental cells. Each contact was padded with equal length flanking regions on both sides and rescaled to 100 bins. Resolution: 5 Kbp.

B, C: Pileup plots of normalized HiC (B) and SMC1 HiChIP (C) contact maps in parental (top) and GSI-resistant (bottom) cells centered around the H3K27ac ChIP-seq peaks with decreased (left), increased (middle) or invariant (right) H3K27ac levels in GSI-resistant compared to parental cells. Each heatmap showing +/- 100 Kbp flanking the center with 5 Kbp resolution.

D, E: Cumulative distribution plots showing differential HiC contact frequency (D) and differential gene expression (E) in GSI-resistant compared to parental cells as a function of whether the connected enhancer changes from super-enhancer (SE) to typical enhancer (TE), remains unchanged, or changes from TE to SE in GSI-resistant compared to parental cells.

F: Normalized HiC contact matrices in parental (top) and GSI-resistant cells (middle), and insulation profile (bottom) at the *MYC* locus (F) showing invariant TAD boundaries.

G: Distances between the *MYC* promoter and super-enhancers E1 and E2 remain unchanged in short-term GSI-treated parental DND41. Left: representative of cells and magnified images for 3-color, *MYC* promoter (yellow)-super-enhancer E1 (magenta), and *MYC* promoter (yellow)-super-enhancer E2 (cyan), from left to right, in parental DND41 treated with DMSO or 125 nM GSI for 24 hours are shown. Location of three 50 Kbp *MYC* promoter (yellow), super-enhancer E1 (magenta) and super-enhancer E2 (cyan) for which Oligopaint probes were designed are marked in Figure 2G. Right: Boxplots of distances between the *MYC* promoter and the closest *MYC* enhancers E1 and E2 probes in the same cell are compared between DMSO (blue, N = 1,652) and GSI-treated (grey, N = 1,323) cells. Mean (+/- S.D.) distance of *MYC* promoter-E1 in DMSO and GSI-treated cells are 0.399 (+/- 0.176) μm, and 0.392 (+/- 0.175) μm, respectively (Student's t-test p-value = 0.1). Mean (+/- S.D.) distance of *MYC* promoter-E2 in DMSO and GSI-treated cells are 0.401 (+/- 0.173) μm, and 0.399 (+/- 0.171) μm, respectively (Student's t-test p-value = 0.6). Blue: DAPI.

H: Selected pathways enriched with genes downregulated in GSI-treated parental cells and re-expressed in GSI-resistant DND41 (see STAR Methods). MSigDB was used for analysis of functional gene annotation.

I: Relative cell growth (CellTiter-Glo) in Cas9-expressing parental (left, DND41-Cas9) and Cas9-expressing GSI-resistant (right, DND41-Res-Cas9) DND41 cells after transduction with control sgRNA (Ctrl) or *MYC*-targeting sgRNA (MYC-KO). Representative data of 3 independent experiments showing mean ± S.D. of 5 technical replicates. p-values: Student's t-test.

Figure S3

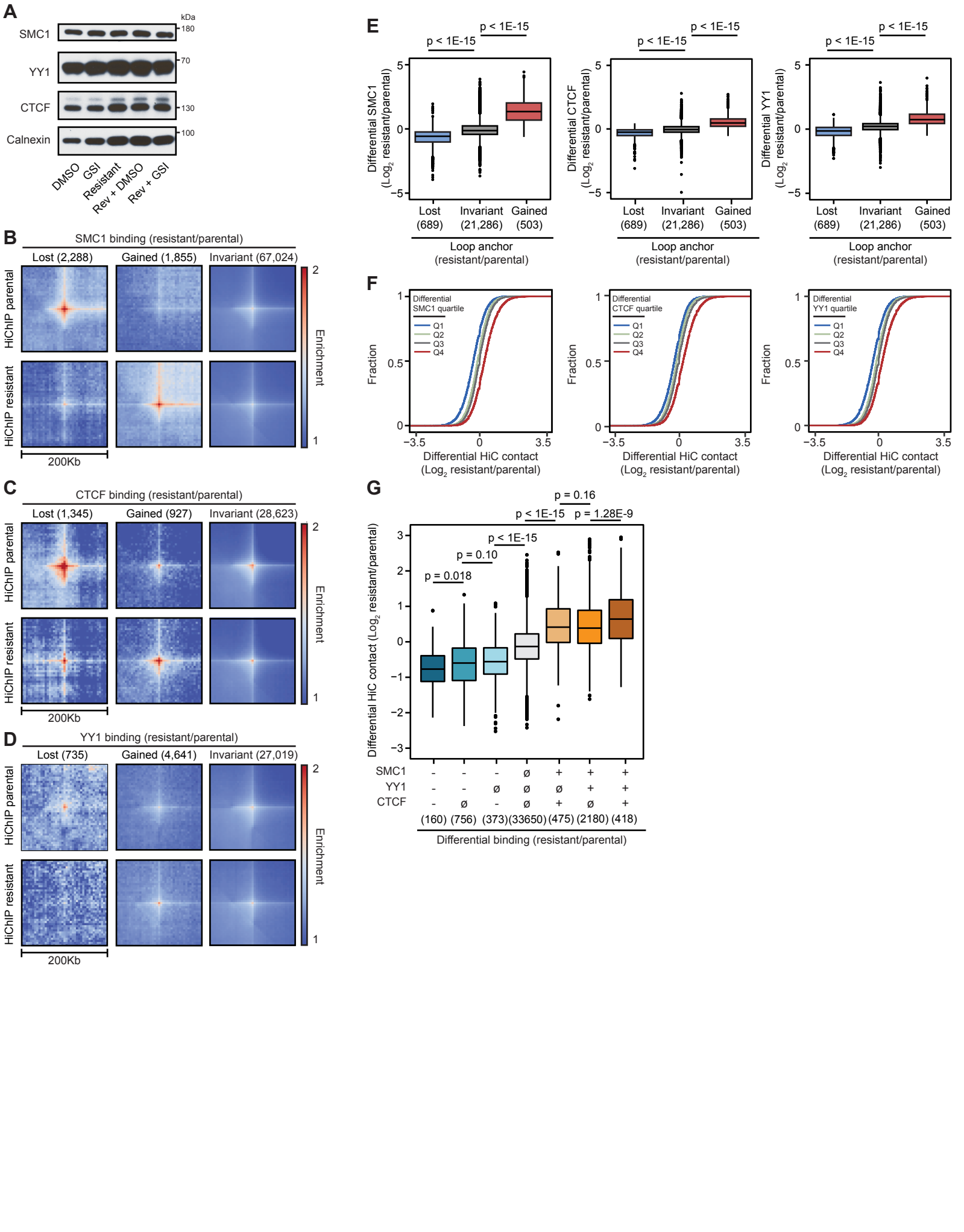
A
kDa
SMC1
180
YY1
70
CTCF
130
Calnexin
100
DMSO
GSI
Resistant
Rev + DMSO
Rev + GSI
B
SMC1 binding (resistant/parental)
Lost (2,288)
Gained (1,855)
Invariant (67,024)
HiChIP parental
HiChIP resistant
Enrichment
200Kb
C
CTCF binding (resistant/parental)
Lost (1,345)
Gained (927)
Invariant (28,623)
D
YY1 binding (resistant/parental)
Lost (735)
Gained (4,641)
Invariant (27,019)
E
p < 1E-15
Differential SMC1 (Log2 resistant/parental)
Differential CTCF (Log2 resistant/parental)
Differential YY1 (Log2 resistant/parental)
Lost (689)
Invariant (21,286)
Gained (503)
Loop anchor (resistant/parental)
F
Differential SMC1 quartile
Differential CTCF quartile
Differential YY1 quartile
Q1
Q2
Q3
Q4
Fraction
Differential HiC contact (Log2 resistant/parental)
G
p = 0.16
p < 1E-15
p = 1.28E-9
p = 0.10
p = 0.018
Differential HiC contact (Log2 resistant/parental)
SMC1
YY1
CTCF
(160) (756) (373) (33650) (475) (2180) (418)
Differential binding (resistant/parental)

Figure S3: SMC1, CTCF and YY1 chromatin binding redistribution coincides with differential loops in GSI-resistant cells. Related to Figure 3.

A: Immunoblot showing invariant SMC1, CTCF and YY1 protein levels in DMSO-treated parental, 24-hour GSI-treated parental, GSI-resistant, DMSO-treated reversed, and 24-hour GSI-treated reversed DND41 cells. Calnexin is a loading control.

B, C, D: Pileup plots of normalized SMC1 HiChIP contact maps in parental (top) and GSI-resistant (bottom) cells centered around the SMC1 (B), CTCF (C) and YY1 (D) peaks with decreased (left), increased (middle) or invariant (right) protein loading in GSI-resistant compared to parental cells. Numbers in parentheses indicate count of differential binding events for each protein. Each heatmap showing +/- 100 Kbp flanking the center with 5 Kbp resolution.

E: Boxplots of SMC1 (left), CTCF (middle) and YY1 (right) loading at the anchors of long-range DNA loops with decreased, increased or invariant interaction frequencies in GSI-resistant compared to parental cells. p-values: Wilcoxon rank sum test.

F: Cumulative distribution plots showing differential HiC contact frequencies in GSI-resistant compared to parental cells as a function of differential SMC1 (left), CTCF (middle) and YY1 (right) levels (log2 resistant/parental) at loop anchors subdivided as quartiles (Q1-4).

G: Boxplots of differential HiC contact frequencies in GSI-resistant compared to parental cells as a function of combinatorial decreased (-), invariant (∅) or increased (+) levels of SMC1, CTCF and YY1. Numbers in parentheses indicate count of binding events for each combination of proteins. p-values: Wilcoxon rank sum test.

Figure S4

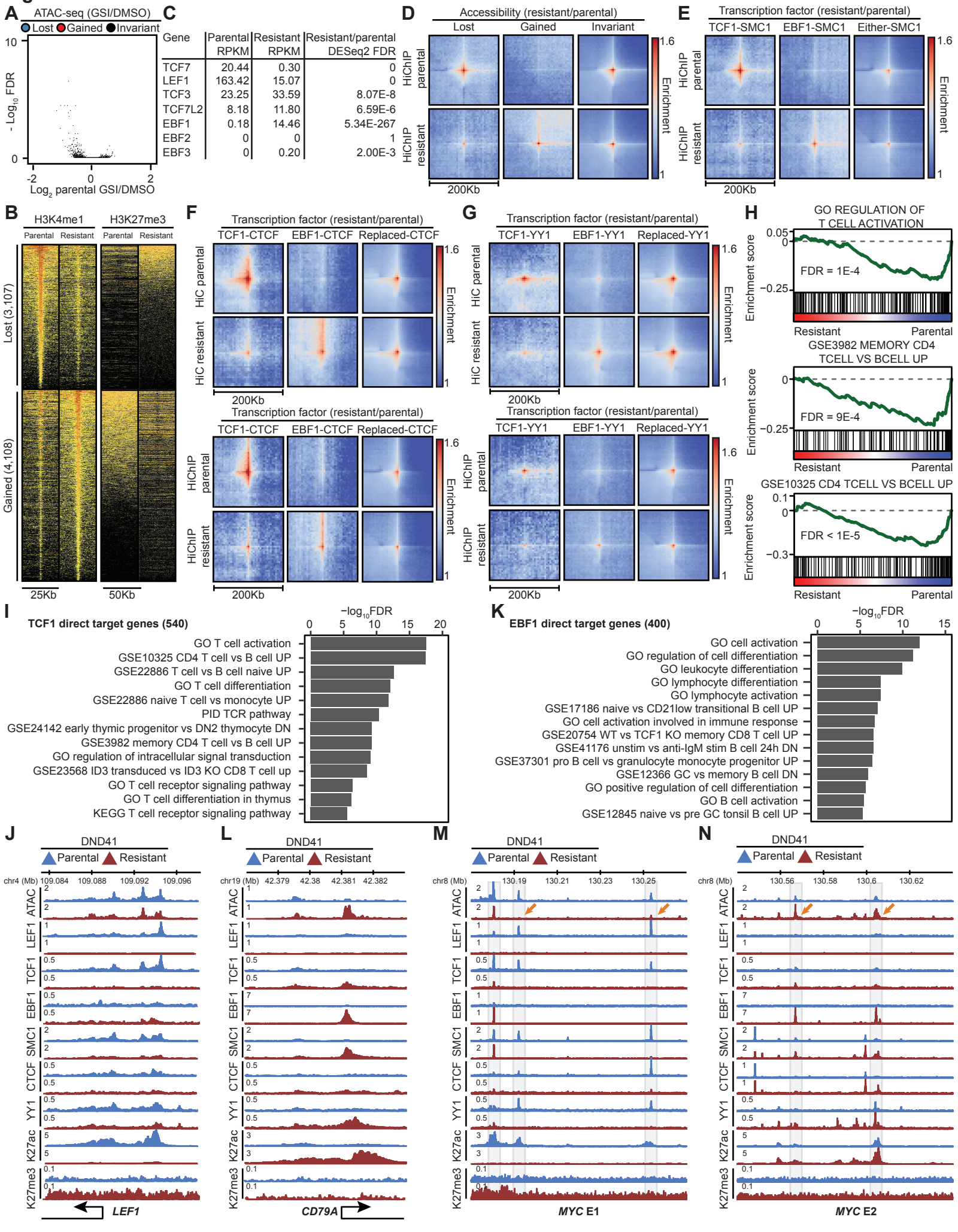
A
ATAC-seq (GSI/DMSO)
Lost Gained Invariant
- Log10 FDR
Log2 parental GSI/DMSO
C
Gene | Parental RPKM | Resistant RPKM | Resistant/parental DESeq2 FDR
TCF7 | 20.44 | 0.30 | 0
LEF1 | 163.42 | 15.07 | 0
TCF3 | 23.25 | 33.59 | 8.07E-8
TCF7L2 | 8.18 | 11.80 | 6.59E-6
EBF1 | 0.18 | 14.46 | 5.34E-267
EBF2 | 0 | 0 | 1
EBF3 | 0 | 0.20 | 2.00E-3
D
Accessibility (resistant/parental)
Lost Gained Invariant
HiChIP parental
HiChIP resistant
Enrichment
200Kb
E
Transcription factor (resistant/parental)
TCF1-SMC1 EBF1-SMC1 Either-SMC1
B
H3K4me1 H3K27me3
Parental Resistant
Lost (3,107)
Gained (4,108)
25Kb 50Kb
F
Transcription factor (resistant/parental)
TCF1-CTCF EBF1-CTCF Replaced-CTCF
HiC parental
HiC resistant
HiChIP parental
HiChIP resistant
200Kb
G
Transcription factor (resistant/parental)
TCF1-YY1 EBF1-YY1 Replaced-YY1
H
GO REGULATION OF T CELL ACTIVATION
FDR = 1E-4
Enrichment score
Resistant Parental
GSE3982 MEMORY CD4 TCELL VS BCELL UP
FDR = 9E-4
GSE10325 CD4 TCELL VS BCELL UP
FDR < 1E-5
I
TCF1 direct target genes (540)
−log10FDR
GO T cell activation
GSE10325 CD4 T cell vs B cell UP
GSE22886 T cell vs B cell naive UP
GO T cell differentiation
GSE22886 naive T cell vs monocyte UP
PID TCR pathway
GSE24142 early thymic progenitor vs DN2 thymocyte DN
GSE3982 memory CD4 T cell vs B cell UP
GO regulation of intracellular signal transduction
GSE23568 ID3 transduced vs ID3 KO CD8 T cell up
GO T cell receptor signaling pathway
GO T cell differentiation in thymus
KEGG T cell receptor signaling pathway
K
EBF1 direct target genes (400)
GO cell activation
GO regulation of cell differentiation
GO leukocyte differentiation
GO lymphocyte differentiation
GO lymphocyte activation
GSE17186 naive vs CD21low transitional B cell UP
GO cell activation involved in immune response
GSE20754 WT vs TCF1 KO memory CD8 T cell UP
GSE41176 unstim vs anti-IgM stim B cell 24h DN
GSE37301 pro B cell vs granulocyte monocyte progenitor UP
GSE12366 GC vs memory B cell DN
GO positive regulation of cell differentiation
GO B cell activation
GSE12845 naive vs pre GC tonsil B cell UP
J
DND41
Parental Resistant
chr4 (Mb)
ATAC LEF1 TCF1 EBF1 SMC1 CTCF YY1 K27ac K27me3
LEF1
L
DND41
Parental Resistant
chr19 (Mb)
CD79A
M
DND41
Parental Resistant
chr8 (Mb)
MYC E1
N
DND41
Parental Resistant
chr8 (Mb)
MYC E2

Figure S4: Differential activity of LEF1/TCF1 and EBF1 orchestrates epigenetic and transcriptomic changes in GSI-resistance. Related to Figure 4.

A: Volcano plot showing ATAC-seq signal fold enrichment (x axis) versus false discovery rate (FDR) (y axis) in parental DND41 cells treated with DMSO or 125 nM GSI for 24 hours. Each point depicts an accessible element, color coded by blue, red, and black based on whether it significantly decreases, increases, or does not change accessibility in GSI-treated parental cells. Significance cutoff: FDR < 1E-5 and log2(fold change) => 1.

B: Heatmaps displaying normalized H3K4me1 (left) and H3K27me3 (right) levels at each of the 3,107 and 4,109 elements with significant decrease (top) or increase (bottom) of accessibility in GSI-resistant compared to parental cells, respectively. Each column of H3K4me1 (H3K27me3) was centered on differentially accessible sites per Figure 4A +/- 12.5 (25) Kbp flanking sequences with 250 bp resolution.

C: Expression of TCF and EBF family members in parental and GSI-resistant cells measured by RNA-seq. FDR was calculated by DESeq2 (see STAR Methods).

D: Pileup plots of normalized SMC1 HiChIP contact maps in parental (top) and GSI-resistant (bottom) cells centered around the accessible elements with significantly decreased (left), increased (middle) or invariant (right) accessibility in GSI-resistant compared to parental cells. Each heatmap showing +/- 100 Kbp flanking the center with 5 Kbp resolution.

E: Pileup plots of normalized SMC1 HiChIP contact maps in parental (top) and GSI-resistant (bottom) cells depicting pairwise contact between accessible elements with loss of TCF1 and SMC1 (left); gain of EBF1 and SMC1 (middle); loss of TCF1 and gain of EBF1 and invariant SMC1 (right) in GSI-resistant cell. Each heatmap showing +/- 100 Kbp flanking the center with 5 Kbp resolution.

F, G: Same as E for CTCF (F) and YY1 (G) on normalized HiC (top) and SMC1 HiChIP (bottom) contact maps.

H: GSEA analysis showing the enrichment of T-cell-related genes versus B-cell-related genes in parental versus GSI-resistant DND41 cells.

I: Selected gene-ontology terms and pathways enriched for TCF1 target genes, which are defined as downregulated genes with loss of TCF1 binding at their promoters or connected distal enhancers during GSI-resistance development (see STAR Methods). MSigDB was used for analysis of functional gene annotation.

J: ATAC-seq, ChIP-seq and Cut&Run tracks showing decreased chromatin accessibility, LEF1, TCF1, SMC1, CTCF, YY1, H3K27ac and H3K4me1 levels and increased H3K27me3 level at the *LEF1* promoter in parental compared to GSI-resistant cells. Bottom track indicating Ensembl gene position.

K: Selected gene-ontology terms and pathways enriched for EBF1 target genes, defined as upregulated genes with gain of EBF1 binding at their promoters or connected distal enhancers in GSI-resistant cells (see STAR Methods). MSigDB was used for analysis of functional gene annotation.

L: ATAC-seq, ChIP-seq and Cut&Run tracks showing increased chromatin accessibility, EBF1, SMC1, YY1, H3K27ac and H3K4me1 levels at the *CD79A* promoter. Bottom track indicating Ensembl gene position.

M: *MYC* super-enhancer E1 loses LEF1, TCF1 and active chromatin marks in GSI-resistant cells. Gray boxes marking elements with differential TCF1/LEF1 and EBF1 levels in parental and GSI-resistant cells. Orange arrows marking differentially accessible elements. Notably, the most 5' element at the super-enhancer E1 region binds EBF1 instead of TCF1 and remains open in GSI-resistant cells.

N: *MYC* super-enhancer E2 gains EBF1 and active chromatin marks in GSI-resistant cells. Gray boxes marking elements with differential TCF1/LEF1 and EBF1 levels in parental and GSI-resistant cells. Orange arrows marking differentially accessible elements.

Figure S5

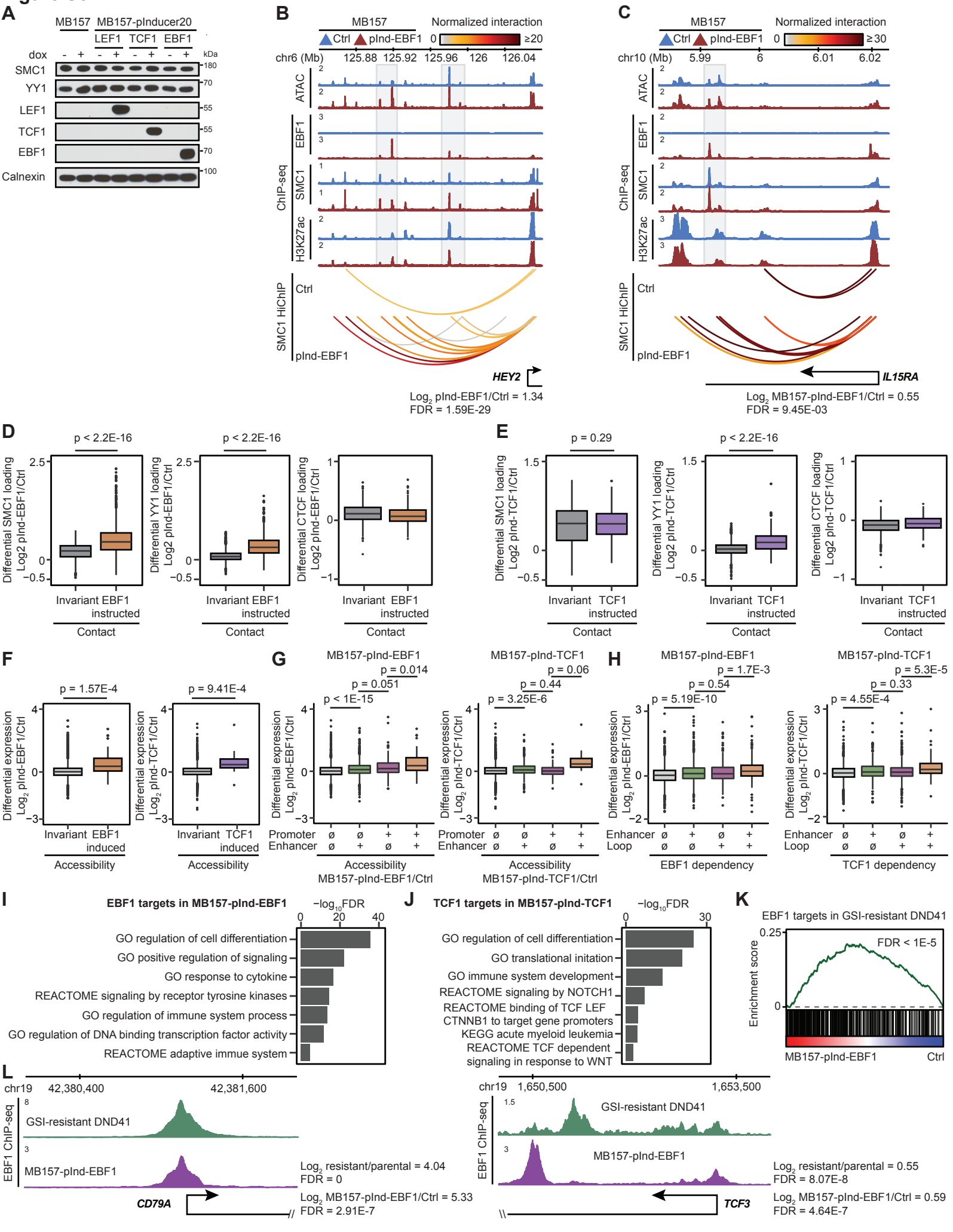
A
MB157
MB157-pInducer20
LEF1
TCF1
EBF1
dox
kDa
SMC1
YY1
LEF1
TCF1
EBF1
Calnexin
180
70
55
55
70
100
B
MB157
Normalized interaction
Ctrl
pInd-EBF1
0
≥20
chr6 (Mb)
125.88
125.92
125.96
126
126.04
ATAC
ChIP-seq
EBF1
SMC1
H3K27ac
SMC1 HiChIP
Ctrl
pInd-EBF1
HEY2
Log2 pInd-EBF1/Ctrl = 1.34
FDR = 1.59E-29
C
MB157
Normalized interaction
Ctrl
pInd-EBF1
0
≥30
chr10 (Mb)
5.99
6
6.01
6.02
IL15RA
Log2 MB157-pInd-EBF1/Ctrl = 0.55
FDR = 9.45E-03
D
p < 2.2E-16
p < 2.2E-16
Differential SMC1 loading Log2 pInd-EBF1/Ctrl
Differential YY1 loading Log2 pInd-EBF1/Ctrl
Differential CTCF loading Log2 pInd-EBF1/Ctrl
Invariant
EBF1 instructed
Contact
E
p = 0.29
p < 2.2E-16
Differential SMC1 loading Log2 pInd-TCF1/Ctrl
Differential YY1 loading Log2 pInd-TCF1/Ctrl
Differential CTCF loading Log2 pInd-TCF1/Ctrl
Invariant
TCF1 instructed
Contact
F
p = 1.57E-4
p = 9.41E-4
Differential expression Log2 pInd-EBF1/Ctrl
Differential expression Log2 pInd-TCF1/Ctrl
Invariant
EBF1 induced
TCF1 induced
Accessibility
G
MB157-pInd-EBF1
MB157-pInd-TCF1
p = 0.014
p = 0.051
p < 1E-15
p = 0.06
p = 0.44
p = 3.25E-6
Differential expression Log2 pInd-EBF1/Ctrl
Differential expression Log2 pInd-TCF1/Ctrl
Promoter
Enhancer
Accessibility
MB157-pInd-EBF1/Ctrl
MB157-pInd-TCF1/Ctrl
H
MB157-pInd-EBF1
MB157-pInd-TCF1
p = 1.7E-3
p = 0.54
p = 5.19E-10
p = 5.3E-5
p = 0.33
p = 4.55E-4
Differential expression Log2 pInd-EBF1/Ctrl
Differential expression Log2 pInd-TCF1/Ctrl
Enhancer
Loop
EBF1 dependency
TCF1 dependency
I
EBF1 targets in MB157-pInd-EBF1
−log10FDR
GO regulation of cell differentiation
GO positive regulation of signaling
GO response to cytokine
REACTOME signaling by receptor tyrosine kinases
GO regulation of immune system process
GO regulation of DNA binding transcription factor activity
REACTOME adaptive immune system
J
TCF1 targets in MB157-pInd-TCF1
−log10FDR
GO regulation of cell differentiation
GO translational initation
GO immune system development
REACTOME signaling by NOTCH1
REACTOME binding of TCF LEF CTNNB1 to target gene promoters
KEGG acute myeloid leukemia
REACTOME TCF dependent signaling in response to WNT
K
EBF1 targets in GSI-resistant DND41
Enrichment score
FDR < 1E-5
MB157-pInd-EBF1
Ctrl
L
chr19
42,380,400
42,381,600
EBF1 ChIP-seq
GSI-resistant DND41
MB157-pInd-EBF1
CD79A
Log2 resistant/parental = 4.04
FDR = 0
Log2 MB157-pInd-EBF1/Ctrl = 5.33
FDR = 2.91E-7
chr19
1,650,500
1,653,500
GSI-resistant DND41
MB157-pInd-EBF1
TCF3
Log2 resistant/parental = 0.55
FDR = 8.07E-8
Log2 MB157-pInd-EBF1/Ctrl = 0.59
FDR = 4.64E-7

Figure S5: Ectopic TCF1 and EBF1 instruct DNA loops and respectively induce T- and B-cell-specific transcriptional programs in TNBC. Related to Figure 5.

A: Immunoblot showing ectopic expression of LEF1, TCF1 and EBF1 and invariant SMC1 and YY1 levels in MB157 cells transduced with pInducer20 plasmids carrying the corresponding genes three days after adding 10 µg/ml doxycycline. Endogenously, MB157 cells do not express these proteins. Calnexin is a loading control.

B, C: EBF1 induces chromatin accessibility and DNA loops in MB157 TNBC. ATAC-seq and ChIP-seq tracks showing increased accessibility, EBF1, SMC1 and H3K27ac levels at distal enhancers connect to *HEY2* (B) or *IL15RA (C)*, which are significantly upregulated in MB157-pInd-EBF1. SMC1 HiChIP arcs displaying normalized significant contacts among enhancers and promoters in MB157 and MB157-pInd-EBF1 (paired t-test p-value 7.05E-8). Bottom track indicating Ensembl gene position, log2 MB157-pInd-EBF1/MB157 expression fold change and FDR as determined by DESeq2.

D, E: Boxplots showing the log2 fold change of SMC1 (left), YY1 (middle) and CTCF (right) levels at elements with significant gain of DNA looping, EBF1 (D) or TCF1 (E) binding, and accessibility in MB157-pInd-EBF1 (D) or MB157-pInd-TCF1 (E) compared to MB157 cells. p-values: Wilcoxon rank sum test.

F: Boxplots showing the log2 fold expression change in genes connected to elements with significant gain of accessibility and EBF1 in MB157-pInd-EBF1 (left) or TCF1 in MB157-pInd-TCF1 (right) compared to MB157 cells. p-values: Wilcoxon rank sum test.

G: Boxplots of log2 gene expression in MB157-pInd-EBF1 (left) or MB157-pInd-TCF1 (right) versus MB157 as a function of combinatorial increased (+) or invariant (∅) accessibility of promoters and connected enhancers. p-values: Wilcoxon rank sum test.

H: Boxplots of log2 gene expression in MB157-pInd-EBF1 (left) or MB157-pInd-TCF1 (right) versus MB157 as a function of connected enhancers' combinatorial increased (+) or invariant (∅) activity and interaction frequency. p-values: Wilcoxon rank sum test.

I, J: Selected gene-ontology terms and pathways enriched for EBF1 (I) or TCF1 (J) target genes, which are defined as upregulated genes with gain of EBF1 (I) or TCF1 (J) binding at their promoters or connected distal enhancers in MB157-pInd-EBF1 (I) or MB157-pInd-TCF1 (J) compared to MB157 cells (see STAR Methods). MSigDB was used for analysis of functional gene annotation.

K: GSEA analysis showing upregulation of EBF1 targets in GSI-resistant DND41 cells (Figure S4K) in MB157-pInd-EBF1 compared to MB157.

L: EBF1 ChIP-seq tracks in GSI-resistant DND41 and MB157-pInd-EBF1 at *CD79A* (left) and E2A-encoding gene *TCF3* (right) promoters showing binding of EBF1 to the same loci in GSI-

resistant DND41 T-ALL and MB157-pInd-EBF1 TNBC cells. Bottom track indicating Ensembl gene positions, log2 expression fold changes and FDRs as determined by DESeq2.

Figure S6

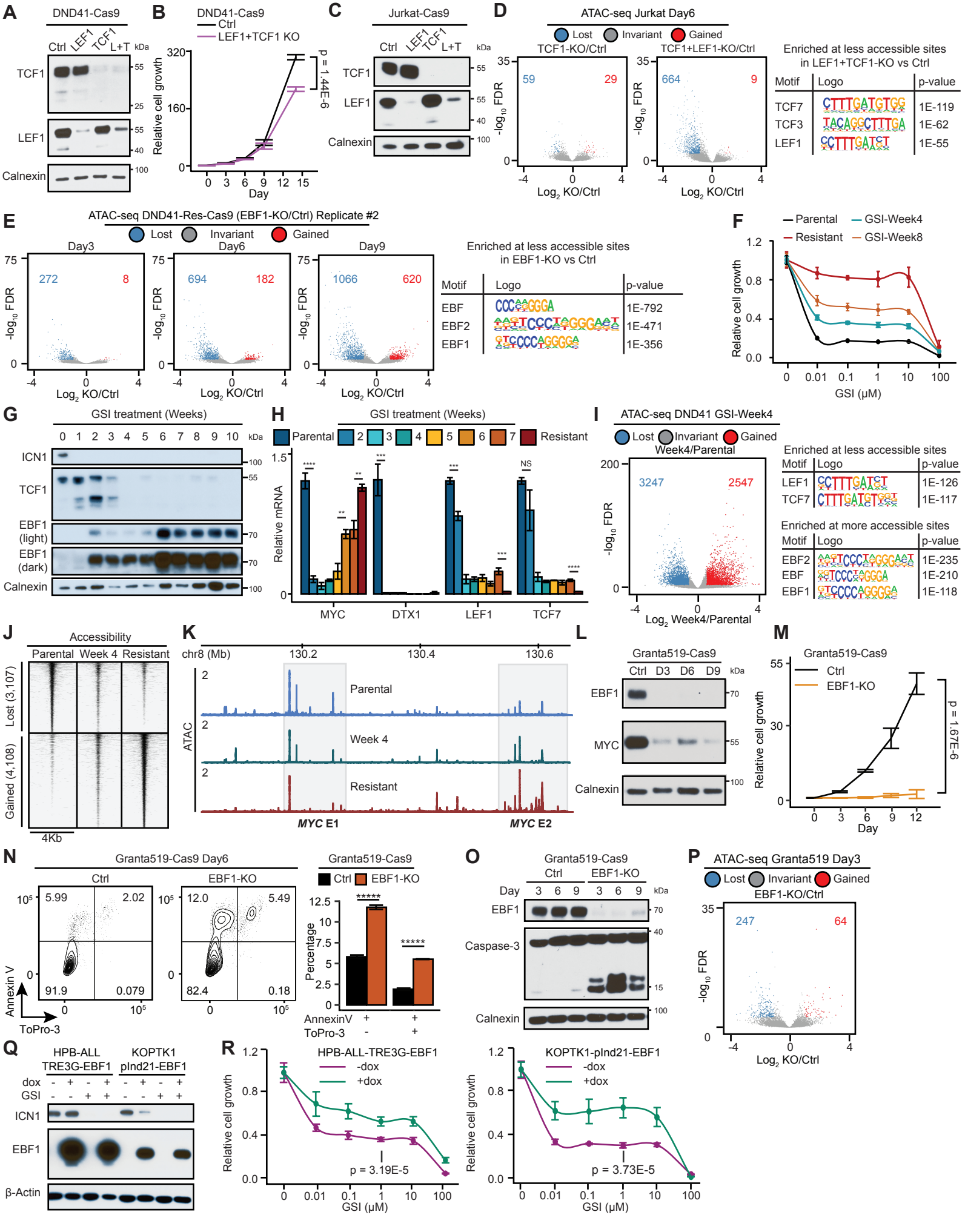
A
DND41-Cas9
Ctrl LEF1 TCF1 L+T kDa
TCF1
LEF1
Calnexin
B
DND41-Cas9
Ctrl
LEF1+TCF1 KO
Relative cell growth
Day
p = 1.44E-6
C
Jurkat-Cas9
Ctrl LEF1 TCF1 L+T kDa
TCF1
LEF1
Calnexin
D
ATAC-seq Jurkat Day6
Lost Invariant Gained
TCF1-KO/Ctrl
TCF1+LEF1-KO/Ctrl
-log10 FDR
Log2 KO/Ctrl
59 29
664 9
Enriched at less accessible sites in LEF1+TCF1-KO vs Ctrl
Motif Logo p-value
TCF7 1E-119
TCF3 1E-62
LEF1 1E-55
E
ATAC-seq DND41-Res-Cas9 (EBF1-KO/Ctrl) Replicate #2
Lost Invariant Gained
Day3 Day6 Day9
272 8
694 182
1066 620
Enriched at less accessible sites in EBF1-KO vs Ctrl
Motif Logo p-value
EBF 1E-792
EBF2 1E-471
EBF1 1E-356
F
Parental GSI-Week4
Resistant GSI-Week8
Relative cell growth
GSI (μM)
G
GSI treatment (Weeks)
0 1 2 3 4 5 6 7 8 9 10 kDa
ICN1
TCF1
EBF1 (light)
EBF1 (dark)
Calnexin
H
GSI treatment (Weeks)
Parental 2 3 4 5 6 7 Resistant
Relative mRNA
MYC DTX1 LEF1 TCF7
I
ATAC-seq DND41 GSI-Week4
Lost Invariant Gained
Week4/Parental
3247 2547
Log2 Week4/Parental
Enriched at less accessible sites
Motif Logo p-value
LEF1 1E-126
TCF7 1E-117
Enriched at more accessible sites
Motif Logo p-value
EBF2 1E-235
EBF 1E-210
EBF1 1E-118
J
Accessibility
Parental Week 4 Resistant
Lost (3,107)
Gained (4,108)
4Kb
K
chr8 (Mb) 130.2 130.4 130.6
ATAC
Parental
Week 4
Resistant
MYC E1
MYC E2
L
Granta519-Cas9
Ctrl D3 D6 D9 kDa
EBF1
MYC
Calnexin
M
Granta519-Cas9
Ctrl
EBF1-KO
Relative cell growth
Day
p = 1.67E-6
N
Granta519-Cas9 Day6
Ctrl EBF1-KO
5.99 2.02 91.9 0.079
12.0 5.49 82.4 0.18
Annexin V
ToPro-3
Granta519-Cas9
Ctrl EBF1-KO
Percentage
AnnexinV
ToPro-3
O
Granta519-Cas9
Ctrl EBF1-KO
Day 3 6 9 3 6 9 kDa
EBF1
Caspase-3
Calnexin
P
ATAC-seq Granta519 Day3
Lost Invariant Gained
EBF1-KO/Ctrl
247 64
-log10 FDR
Log2 KO/Ctrl
Q
HPB-ALL TRE3G-EBF1
KOPTK1 pInd21-EBF1
dox
GSI
ICN1
EBF1
β-Actin
R
HPB-ALL-TRE3G-EBF1
-dox
+dox
p = 3.19E-5
KOPTK1-pInd21-EBF1
-dox
+dox
p = 3.73E-5
Relative cell growth
GSI (μM)

Figure S6: Loss of EBF1 and LEF1/TCF1 reduces chromatin accessibility in transformed B and T cells. Related to Figure 6.

A: Immunoblot showing reduction of TCF1 and LEF1 protein levels in Cas9-expressing parental DND41 (DND41-Cas9) cells three days post transduction with LEF1-targeting (LEF1-KO), TCF1-targeting (TCF1-KO) or both LEF1- and TCF1-targeting (LEF1+TCF1-KO) sgRNAs compared to control sgRNA (Ctrl). Calnexin is a loading control.

B: Relative cell growth of (CellTiter-Glo) Ctrl and LEF1+TCF1-KO DND41-Cas9. Representative data of 3 independent experiments showing mean ± S.D. of 5 biological replicates. Student's t-test p-value: 1.44E-6.

C: Immunoblot showing reduction of TCF1 and LEF1 protein levels in Cas9-expressing Jurkat E6-1 (Jurkat-Cas9) cells three days post transduction with LEF1-targeting (LEF1-KO), TCF1-targeting (TCF1-KO) or both LEF1- and TCF1-targeting (LEF1+TCF1-KO) sgRNAs compared to control sgRNA (Ctrl). Calnexin is a loading control.

D: Volcano plots showing ATAC-seq signal fold enrichment (x axis) versus false discovery rate (FDR) (y axis) in Jurkat-Cas9 TCF1-KO (left) and LEF1+TCF1-KO (right) compared to Ctrl. Each point depicts an accessible element. Elements with significantly decreased or increased accessibility in TCF1-KO or LEF1+TCF1-KO cells are marked in blue and red, respectively. Significance cutoff: DESeq2 FDR < 1E-3 and log2(fold change) => 1. Right table showing HOMER motif enrichment at the sequences with significantly decreased accessibility in LEF1+TCF1-KO compared to Ctrl.

E: Volcano plot showing ATAC-seq signal fold enrichment (x axis) versus false discovery rate (FDR) (y axis) in the second biological replicate of EBF1-KO versus Ctrl GSI-resistant DND41 cells three (left), six (middle) or nine (right) days post sgRNA transduction. Each point depicts an accessible element. Elements with significantly decreased or increased accessibility in EBF1-KO cells are marked in blue and red, respectively. Significance cutoff: DESeq2 FDR < 1E-3 and log2(fold change) => 1. Right table showing HOMER motif enrichment at the sequences with significantly decreased accessibility in EBF1-KO compared to Ctrl.

F: Relative cell growth (CellTiter-glo) of parental, four-week-GSI-treated, eight-week-GSI-treated and GSI-resistant (> 12 weeks) DND41 cells plated with the indicated doses of GSI for 6 days. Live cells among four-week- and eight-week-GSI-treated cells were FACS-sorted prior to plating. Representative experiment of 2 independent biological replicates with 5 technical replicates per dose.

G: Time-course immunoblot showing ICN1 inhibition, rapid TCF1 decrease, and gradual EBF1 increase in the FACS-sorted live cells during 10 weeks of GSI treatment. Calnexin is a loading control.

H: Time-course qRT-PCR showing *MYC* expression dynamics and *DTX1*, *LEF1* and *TCF7* repression in the FACS-sorted live cells during GSI-resistance acquisition. Student's t-test p-value: **p < 5E-3, ***p < 5E-4, ****p < 1E-4, NS p > 0.05.

I: Left: volcano plot showing ATAC-seq signal fold enrichment (x axis) versus false discovery rate (FDR) (y axis) in four-week-GSI-treated versus parental DND41 cells. Each point depicts an accessible element. Elements with significantly decreased or increased accessibility in four-week-GSI-treated cells are marked in blue and red, respectively. Significance cutoff: DESeq2 FDR < 1E-5 and log2(fold change) => 1. Right: table showing HOMER motif enrichment at the sequences with significantly increased or decreased accessibility in four-week-GSI-treated compared to parental cells.

J: heatmaps displaying normalized ATAC-seq signal in parental, four-week-GSI-treated and resistant cells at each of the 3,107 and 4,109 elements with significantly decreased (top) or increased (bottom) accessibility in GSI-resistant compared to parental cells, respectively. Each column was centered on differentially accessible sites per Figure 4A +/- 2 Kbp flanking sequences. Bin size: 50 bp.

K: *MYC* super-enhancer E1 and E2 (grey boxes) partially loses and gains chromatin accessibility in four-week-GSI-treated cells, respectively.

L: Immunoblot showing EBF1 and MYC proteins in Cas9-expressing mantle cell lymphoma Granta519 (Granta519-Cas9) cells three, six and nine days post transduction with control (Ctrl) or EBF1-targeting (EBF1-KO) sgRNA. Calnexin is a loading control.

M: Relative cell growth (CellTiter-Glo) in Ctrl and EBF1-KO Granta519-Cas9. Representative data of 3 independent experiments showing mean ± S.D. of 5 technical replicates. Student’s t-test p-value: 1.67E-6.

N: Flow cytometry plots (left) and quantification (right) of cell apoptosis and death measured by Annexin V and ToPro-3 staining. Ctrl and EBF1-KO Granta519-Cas9 were sorted three days post lentiviral transduction and cultured for three days. Representative experiment of 3 biological replicates with 5 technical replicates. Student’s t-test p-value: ***** p < 1E-5.

O: Immunoblot showing loss of EBF1 induces cell apoptosis measured by cleaved Caspase-3 in unsorted EBF1-KO Granta519-Cas9 three, six, and nine days post lentiviral transduction. Calnexin is a loading control.

P: Volcano plot showing ATAC-seq signal fold enrichment (x axis) versus false discovery rate (FDR) (y axis) in EBF1-KO versus Ctrl Granta519-Cas9 cells three days post sgRNA transduction. Each point depicts an accessible element. Elements with significantly decreased or increased accessibility in EBF1-KO cells are marked in blue and red, respectively. Significance cutoff: DESeq2 FDR < 1E-3 and log2(fold change) => 1.

Q: Immunoblot showing ICN1 and ectopic EBF1 expression levels in Notch-addicted T-ALL HPB-ALL and KOPTK1 cells transduced with TRE3G-EBF1 and pINDUCER21-EBF1 plasmids, respectively. Doxycycline: 0.5 µg/mL for 72 hours; GSI: 1 µM for 24 hours. Representative of two independent biological replicates. β-Actin is a loading control.

R: Relative cell growth (CellTiter-glo) of HPB-ALL-TRE3G-EBF1 and KOPTK1-pInd21-EBF1 cells plated with the indicated doses of GSI with or without 0.5 µg/mL doxycycline for 6 days. Representative experiment of 2 independent biological replicates with 5 technical replicates per dose.

Figure S7

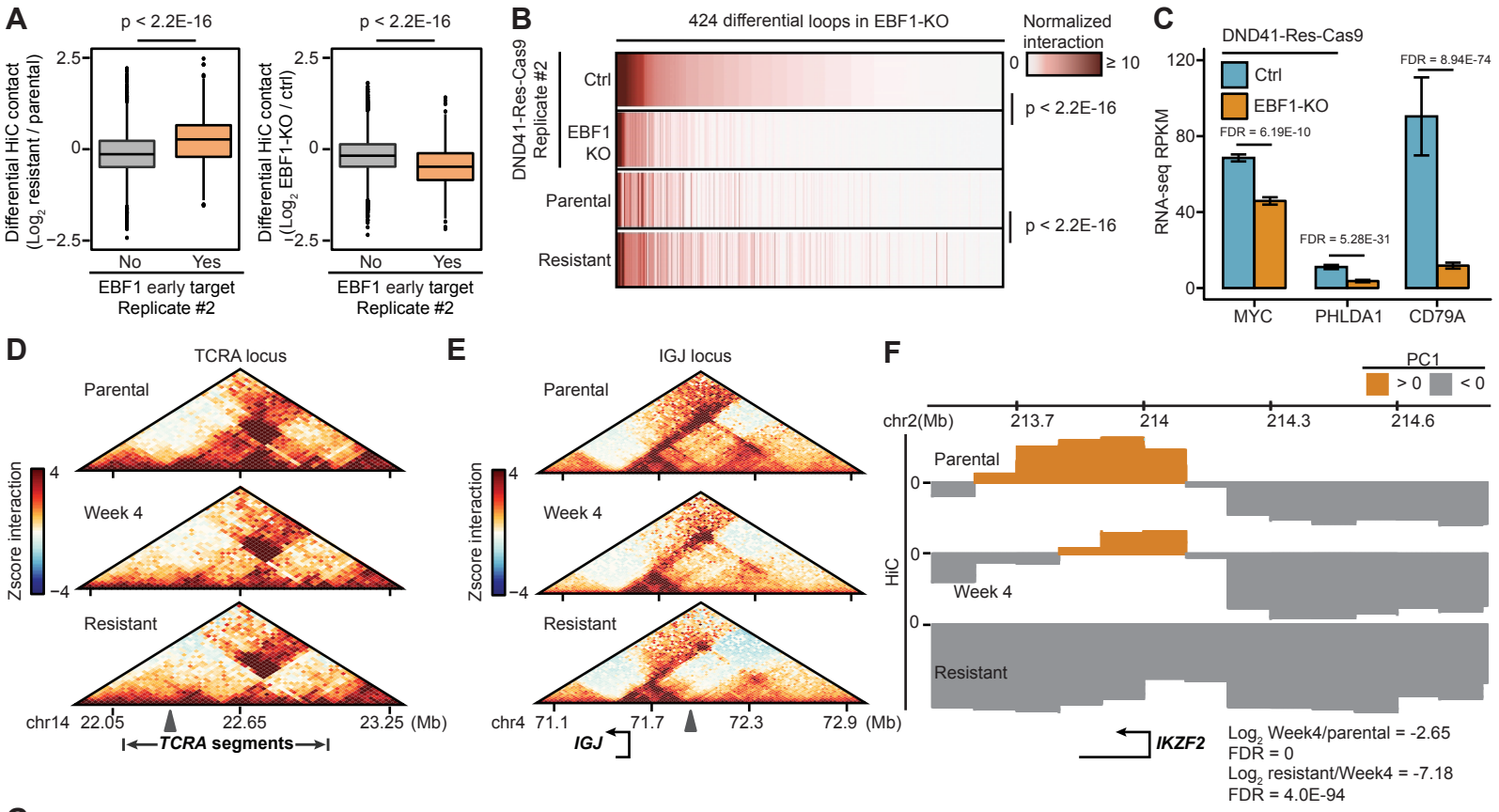

G

Gene	$Log_2(\frac{Week4}{Parental})$	Week4/parental DESeq2 FDR	$Log_2(\frac{Resistant}{Week4})$	Resistant/Week4 DESeq2 FDR	$Log_2(\frac{Resistant}{Parental})$	Resistant/parental DESeq2 FDR	$Log_2(\frac{EBF1\text{-}KO}{Ctrl})$	EBF1-KO/ctrl DESeq2 FDR	$Log_2(\frac{EBF1\text{-}KO}{Ctrl})_{Rep\#2}$	EBF1-KO/ctrl Rep#2 DESeq2 FDR
NOTCH1	-1.41	1.29E-190	-1.58	5.88E-61	-3.02	4.32E-285	-0.083	0.34	-0.15	0.82
GATA3	-0.44	4.67E-9	-0.70	1.10E-9	-1.16	1.38E-33	-0.39	3.14E-10	-0.46	0.001
TCF3	-0.39	4.74E-11	0.96	7.80E-20	0.55	8.07E-8	-0.084	0.39	-0.40	0.013

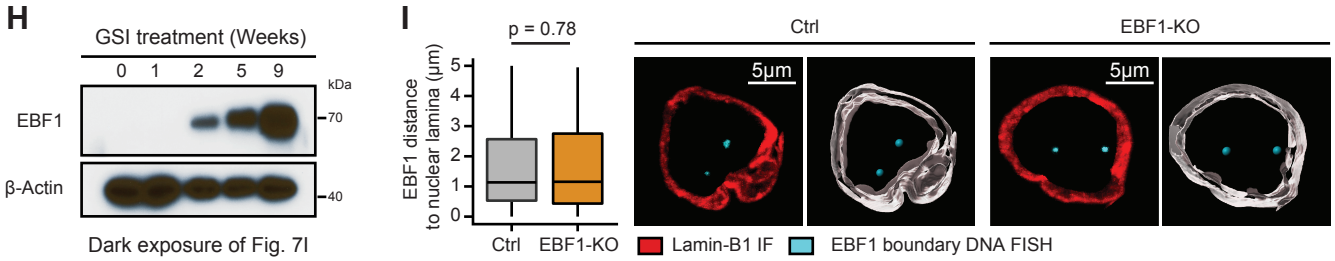

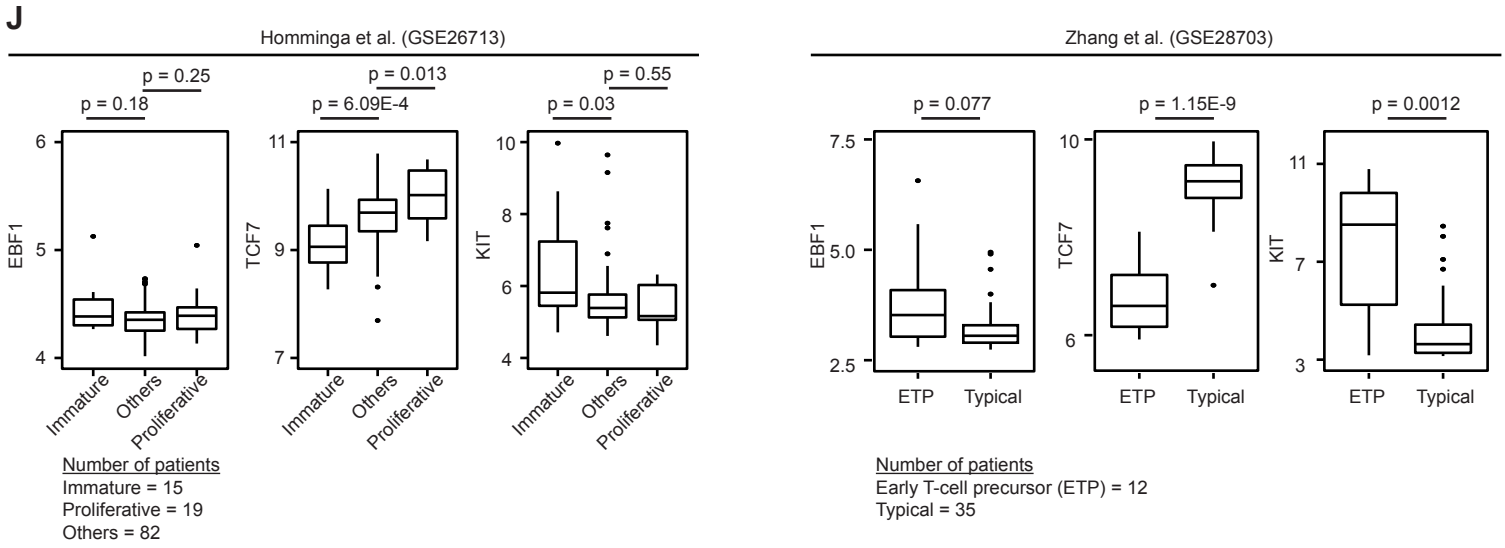

Figure S7: EBF1 and TCF7 expression levels are associated with immature and mature T-ALL subtypes, respectively. Related to Figure 7.

A: Boxplots showing the log2 fold change of normalized HiC contact frequencies in GSI-resistant versus parental DND41 (left) and EBF1-KO versus Ctrl DND41-Res-Cas9 (right, second biological replicate) as a function of whether GSI-resistant accessible elements are EBF1 early targets. p-values: Wilcoxon rank sum t-test.

B: Heatmaps showing normalized HiC interactions, from top to bottom, in the second biological replicate of Ctrl or EBF1-KO DND41-Res-Cas9; and parental or GSI-resistant DND41. Each column is a loop connected to EBF1 early targets with decreased contact frequency in EBF1-KO versus Ctrl DND41-Res-Cas9 (log2 fold change < -0.5). Rows are sorted in descending order of contact frequencies in Ctrl DND41-Res-Cas9. p-values: paired t-test.

C: Expression of *MYC*, *CD79A* and *PHLDA1* in parental and GSI-resistant cells measured by RNA-seq in Ctrl or EBF1-KO DND41-Res-Cas9. FDR: DESeq2.

D, E: Normalized HiC contact matrices in parental (top), four-week-GSI-treated (middle) and GSI-resistant cells (bottom) showing gradual loss and gain of TAD boundary insulation potential at T-cell receptor alpha (*TCRA*) (D) and Immunoglobulin J chain (*IGJ*) (E) loci. Gray arrows: differential boundaries (see STAR Methods).

F: The first principal component (PC1) values of HiC contact Pearson correlation matrices at the *IKZF2* locus in parental, four-week-GSI-treated and GSI-resistant cells showing gradual compartment switching from A (>0) to B (<0) (see STAR Methods). Bottom track indicating *IKZF2* gene position, expression fold change and FDR were determined by DESeq2.

G: Known positive and negative EBF1 regulators are differentially expressed in parental, four-week-GSI-treated and GSI-resistant cells, but not in EBF1-KO Cas9-expressing GSI-resistant DND41 cells (DND41-Res-Cas9). Log2 fold change and FDR for gene expression were determined by DESeq2.

H: Dark exposure of Figure 7I showing gradual increase of EBF1 expression in DND41 during GSI treatment.

I: Distances between *EBF1* and Lamin-B1-marked nuclear envelope do not significantly change in EBF1-KO DND41-Res-Cas9 compared to Ctrl. Left: boxplots of the closest distance between *EBF1* probe and nuclear lamina in the same cell comparing 95 and 99 nuclei in Ctrl and EBF1-KO cells. Mean (+/- S.D.) distance in Ctrl and EBF1-KO cells are 1.61 (+/- 1.41) μm, and 1.67 (+/- 1.46) μm, respectively (Wilcoxon p-value = 0.78). Representative Ctrl (Middle) and EBF1-KO (right) DND41-Res-Cas9 cells showing *EBF1* remains at the nuclear interior six days post sgRNA lentiviral transduction.

J: *EBF1* and *TCF7* (gene encoding for TCF1) expression levels are positively and negatively associated with immature/early thymic progenitor (ETP) T-ALL subtypes, respectively. Normalized gene expression of *EBF1*, *TCF7* and *KIT* from two independent T-ALL patient cohorts GSE26713 and GSE28703 (Homminga et al., 2011; Zhang et al., 2012).